RSC Advances

ROYAL SOCIETY OF CHEMISTRY

www.rsc.org/advances

Journal Name

ARTICLE

Received 00th January 20xx,

Accepted 00th January 20xx

DOI: 10.1039/x0xx00000x

www.rsc.org/

A multi-scale molecular dynamics simulation of PMAL facilitated delivery of siRNA

Jipeng Li,[a] Yiyun Ouyang,[a] Xian Kong,[a] Jingying Zhu,[a] Diannan Lu*[a] and Zheng Liu*[a]

The capability of silencing genes makes small interfering RNA (siRNA) appealing for curing fatal diseases such as cancer and viral infection. In present work, we chosen a novel amphiphilic polymer, PMAL (Poly (maleic anhydride-alt-1-decene) substituted with 3-(Dimethylamino) propylamine), as siRNA carrier, and conducted steered molecular dynamics simulations, in together with traditional molecular dynamics simulations, to explore how PMAL facilitates the delivery of siRNA. It was shown that the participation of PMAL reduced the energy barrier for siRNA to penetrate lipid bilayer membrane, as confirmed by the experiment. The simulation of the transmembrane process revealed that PMAL can punch on lipid bilayer and form a channel for siRNA delivery. The monitoring of the structural transition further showed the targeting of siRNA through the attachment of PMAL encapsulating siRNA to lipid membrane. The delivery of siRNA was facilitated by the hydrophobic interaction between PMAL and lipid membrane, which favored the dissociation of the siRNA-PMAL complex. The above simulation established a molecular insight of the interaction between siRNA and PMAL and was helpful for the design and applications of new carrier for siRNA delivery.

Introduction

Small interfering RNA (siRNA) has attracted broad interests in exploring its potential application in gene therapy for fatal diseases[1-3] since Tuschl et al. firstly published their celebrated proof-of-principle experiment demonstrating that synthetic siRNA could achieve sequence-specific gene knockdown in mammalian cell line[4]. Great efforts have been made to improve siRNA therapeutics for various diseases, including viral infections[5] and cancer[6]. However, the naked siRNA is vulnerably degraded by endogenous enzymes, and is too large (~13 kDa) and too negatively charged to cross cellular membranes. Thus a safe and effective delivery method is pursued for the therapeutic application of siRNA.

Non-viral siRNA delivery carriers, including liposomes, lipid-like materials, polymers and nanoparticles, have been extensively attempted because of their proven advantages in terms of ease of synthesis, low immune response and safety. Felgner et al.[7] firstly succeeded in delivering both DNA and RNA into mouse, rat and human cell lines with the assistance of cationic lipid N-[1-(2,3-dioleyloxy)propyl]-N,N,N trimethyl ammonium chloride (DOTMA). Morrissey[8] found that nucleic acid-lipid particle (SNALP), which is composed of siRNA and liposome, can be administered into mice to inhibit duplicating of HBV.

Cationic polymers with linear or branched structure can serve as efficient transfection agents because of their ability to bind and condense large negatively charged nucleic acid into stable nanoparticles. Polymers of this kind including PEI[9, 10], cyclodextrin[11], chitosan[12] have been examined for siRNA delivery. "Tat peptide" can form complex with siRNA and penetrate cell membrane[13]. Dong et al[14] reported lipopeptide nanoparticles as potent and selective siRNA carriers with a wide therapeutic index. From above efforts, it is concluded an ideal polymer carrier for siRNA delivery should have following capabilities: 1) forming a stable complex with nucleic acids to maintain its stability in biological solution, 2) hiding from the host immune systems, 3) penetrating into cell membrane, and 4) dissociating and releasing siRNA once localized within cells.

Amphiphilic polymers that form complex with siRNA via electrostatic interaction are able to penetrate lipid bilayer membrane via hydrophobic interaction and thus promising for siRNA delivery. Zeng et al.[15] designed and synthesized a new class of dendronized peptide polymers and demonstrated its capability of siRNA delivery. Forbes[16] studied polycationic nanoparticles synthesized using the cationic monomer 2-(diethylamino)ethyl methacrylate and other monomer to enhance stability and biocompatibility. An improved gene knockdown was achieved using AllStarts Hs Cell Death siRNA or AllStars Mm/Tn Cell Death siRNA. Dahlman et al.[17] showed that polymeric nanoparticles made of low-molecular-weight polyamines and lipids can deliver siRNA to endothelial cells with high efficiency. Given above results, the mechanism of cationic polymer-assisted siRNA delivery at molecular level is not fully understood.

[a] *Department of Chemical Engineering, Tsinghua University, Beijing 100084, China*
Electronic Supplementary Information (ESI) available: [details of any supplementary information available should be included here]. See DOI: 10.1039/x0xx00000x

Molecular simulations have been applied to probe the interaction of siRNA and polymer and their effects on the complex stability and structure[18]. Ouyang et al.[19] concluded that dendrimer of higher molecular weight and a lower pH favors a more stable complex with siRNA. Karatasos et al.[20] also examined the effect of pH and size of dendrimer on its complexation with siRNA. The interactions between G4 and G5-G6 with siRNA were totally different. Jensen et al.[21] found that the size of PAMAM G7 drendrimer changed little during the complexation with siRNA, an exothermic process confirmed by both experiments and MD simulation. Ouyang et al.[22] displayed the process details of the complexation of polymer with siRNA. Sun et al.[23] showed that lipid-modified PEIs formed more compact and stable complex with siRNA. Up to date, the transport of polymer-siRNA complex through lipid membrane is, however, rarely reported.

With the appreciation of the potential of maleic anhydride based copolymers that is approved by US FDA (http://www.fda.gov), we directed our efforts to examine its potential for siRNA delivery. The objective of the present study is to establish a molecular insight of transmembrane process of siRNA with the aid of PMAL. We firstly constructed a coarse-grained PMAL model on the basis of an all-atomic MD simulation of PMAL. Then complex consisting of siRNA and PMAL was pulled through membrane with steered molecular simulation and umbrella sampling was employed to get the potential of mean force. The formation and dissociation of PMAL-siRNA complex during the transportation towards and across liposome was monitored so to provide the molecular details and mechanism underlying the transportation. We also performed experiments confirming PMAL facilitated transportation of siRNA to liposome.

Models and Simulation Methods

Models

All-atom PMAL model. To obtain coarse-grained model of PMAL[24], we firstly established all-atom model of PMAL in water. One PMAL polymer consists of 52 repeating units and 3278 atoms. The force field parameters for PMAL atoms are based on the Charmm 27 force field (The topology file for PMAL is given in the SI).

Coarse-grained model of PMAL. Coarse-grained (CG) model of PMAL was built based on all-atomic PMAL and the Martini force field[25]. Six heavy Martini particles were used to represent one PMAL unit, and the relationship between all-atom and coarse-grained model was descripted in Figure 1(middle) and Figure S1 in supporting information. Then MINN's procedure[26] was applied to obtain reasonable information of bond lengths, angle and dihedrals, which were given in SI (Figure S2). The target overlap ratio was set to 0.6, which satisfies not only the needs of siRNA delivery but also the correctness of CG model. The obtained CG model of PMAL was given in Figure 1 (right) with a micelle-like structure, whose hydrophobic groups are inner while hydrophilic groups (charged groups) are outer.

Coarse-grained model of siRNA and lipids. The target siRNA in this study has the following sequence: 5'-CAUGUGAUCGCG CUUCUCGUU-3', which is used extensively to silence green

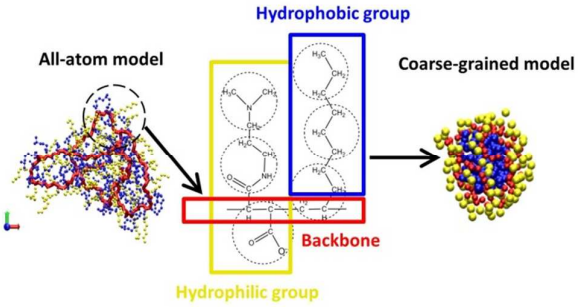

Figure 1. All-atom and coarse-grained PMAL model.

Red: atoms or coarse-grained beads in backbone; Blue: atoms or coarse-grained beads in hydrophobic side chains; Yellow: atoms or coarse-grained beads in hydrophilic (charged) side chains.

fluorescence protein. A siRNA duplex is composed of 42 nucleotides carrying a total charge of -40e in a fully de-protonated state. Because 21bp CG siRNA was still too large to simulate, a 12bp CG duplex carrying a net charge of -22e was used in our study (Figure 2 (a) and (b)). Two kinds of lipids, neutral DPPC (1,2-Dipalmitoyl-sn-glycero-3-phosphocholine) and negatively charged DPPG (1,2-Dipalmitoyl-sn-glycero-3-phosphoglycerol, sodium salt) were used. The structures of lipid molecules were given in Figure 2(f). Four water molecules were treated together as one coarse-grained bead with a mass of 72 amu.

Complexation of siRNA and PMAL in water. In order to obtain a stable structure of aqueous siRNA-PMAL complex, simulated annealing simulation with 10 repeating period was conducted from initial configuration, as shown in Figure 2(b). The stable complex composed of siRNA and PMAL was shown in Figure 2(c). The initial configurations for siRNA and PMAL-siRNA complex through lipid bilayer were given in Figure 2(d) and (e), respectively.

Simulation Details

All simulations were conducted with the MD engine GROMACS[27] and VMD was used to visualize the systems[28].

Simulated annealing MD simulation for all-atom model. The PMAL was solvated with 23,185 SPC/E water molecules in a rhombic dodecahedral box. Annealing simulations was conducted to obtain a stable structure, which was shown in Figure 1(left), and was used as a starting point for coarse-grained (CG) model of PMAL. 20ns simulation was performed to provide average distribution of bond and angle that was used to build model for the CG model of PMAL.

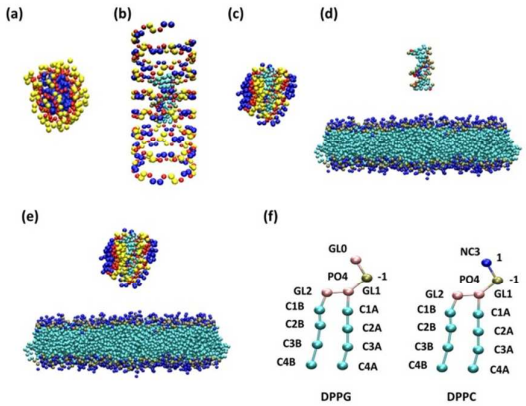

Figure 2. (a) Stable structure of PMAL; (b) Initial configuration of siRNA and PMAL;(c) Stable structure of complex(siRNA-PMAL); (d) Initial configuration of siRNA and membrane to conduct pulling simulation; (e) Initial configuration of complex and membrane to conduct pulling simulation; (f) Structure of DPPC and DPPG;

Simulated annealing MD simulation for coarse-grained model. The coarse grained PMAL was solvated with 6,391 martini water molecules in cubic box with 9.3nm in length for each side. After several repeating annealing runs, 20-ns equilibrium molecular dynamics simulation was performed to get a series of stable structures of PMAL in water. Bond and angle distributions of all-atom model and CG model were compared (details are given in SI). Then we adjusted the bond parameters of CG model and repeated the former process until ratio of overlap reached 0.6.

Traditional MD simulation for complex. PMAL and siRNA were put into a cubic box with 13nm in length for each side. The initial configurations for complex through membrane are given in Figure 2(b). In order to obtain a stable structure of complex composed of siRNA and PMAL in water, simulated annealing simulation with 10 repeating runs was conducted from initial configuration. The stable complex composed of siRNA and PMAL was shown in Figure 2(c).

Pulling simulation for transmembrane process. Stable complex or bare siRNA was put into the box (Figure 2(d) or (e)) containing lipid membrane in center whose normal direction is the z direction. The lipid bilayer was composed of 483 DPPC and 161 DPPG molecules, which were equally distributed in each monolayer. The mass center distance between complex and lipid membrane was set about 7 nm. Because the real mammal cell membrane carries negative charges, the lipid bilayer membrane with ratio of DPPC (neutral) and DPPG (negative) was set as 3:1 to mimic mammal cell membrane in many previous reports[29-31], which was also used in the present work. 43,468 water and 138 charged CG counterions were added to solvate system and to achieve electric neutrality, respectively. The pulling force 1,000 kJ/(mol nm^2) was applied to perform pulling simulation with a rate of pulling of 10^{-5} nm/ps. The trajectory of pulling was saved and used as windows for umbrella simulation. Then each of 91 sampling windows ran 90 ns with a timestep of 30 fs. Potential of mean force curves were obtained using umbrella sampling[32] and wham method[33]. NPT ensemble was chosen and temperature was maintained at 310K and pressure was controlled at 1 a.t.m using Berendsen method[34]. Lennard-Jones potential forces were shifted smoothly from 0.9nm to 1.2nm. The screened electrostatic Coulombic interactions were processed using PME method[35, 36] with a short range cutoff of 1.4nm.

Analytic methods

Lipid order parameter, S_Z , which reflects the orientation and the order of lipid molecule perpendicular to lipid bilayer normal, is defined as

$$S_Z = \frac{3}{2}\left\langle \cos^2 \theta_Z \right\rangle - \frac{1}{2}$$

in which θ_Z is the angle between the vector from C1A to C3A of lipid and z-axis. S_Z ranges from -0.5 to 1.0. $S_Z = 1.0$ means lipid molecule is perfectly parallel or anti-parallel to z-axis, i.e., lipid molecules is perpendicular to the bilayer normal. $S_Z = -0.5$ means lipid molecule is perpendicular to z-axis.

Plane coefficients (γ), denoted as root mean squares of the z coordinates of certain particles, is defined as

$$\gamma = \sqrt{\frac{1}{N}\sum_{i=1}^{N}(Z_i - \bar{Z})^2}$$

in which Z_i was the z-coordinate value of the fourth bead (C4A and C4B) of lipid molecule i in z-axis, $\bar{Z}$ was the average of z-coordinate value of the fourth beads of all lipid molecule, and N was number of all beads that participate the calculation. γ reflects the flatness of the bilayer.

Materials and experimental methods

DPPC, DPPG and PMAL were purchased from Sigma-Aldrich. Complementary siRNA chains with fluorescence label were purchased from Sango Biotech (Shanghai, China).

DPPC and DPPG with a given ratio were dissolved in chloroform. Lipid membrane was obtained after chloroform volatilization. Then water was added to get lipid solution with a final concentration of 5mg/mL. The solution was filtered through filter membrane with pore size 1μm for 11 times to get liposome.

The fabrication of double chains siRNA was performed by temperature annealing. Firstly, siRNA solution was denatured at temperature 95 ℃ for 5 min. And then the solution was cooled to room temperature to form double strand siRNA. The final concentration of siRNA was 100μM.

The concentration of stock solution of PMAL was 1mM. The stock solution of PMAL was diluted to 100μM before mixing with siRNA solution. To form complex, siRNA solution was mixed for 1 hour or a longer time with PMAL solution with molar ratio of 1: 1. Then complex or solely siRNA solution was added into liposome solution. After 4 hours, the sample was taken and observed by using laser scanning confocal microscope.

Results and Discussion

The PMAL facilitated transport of siRNA: a free energy perspective

Firstly, we simulated the transmembrane of bare siRNA and siRNA-PMAL complex. The free energy as function of distance between the center-of-mass (COMs) of lipid bilayer and siRNA or siRNA-PMAL complex is given in Figure 3.

It is shown in Figure 3(a) that when bare siRNA is pulled across DPPC bilayer, the free energy is above zero. When the COMs between lipid membrane and siRNA is smaller than 2 nm, notable repulsive interaction occurs and an energy barrier of about 100

kJ/mol exists. This agrees with that simulated by Lin et al.[37]. Though siRNA carries negative charge (-22e), no net columbic interactions is observed. This is because lipid membrane is neutral and thus Van der waals force dominates the transmembrane process. Interestingly, for PMAL-siRNA complex, the free energy profile appears no energy barrier for the complex to penetrate DPPC membrane. Moreover, the energy valley for the complex is deeper compared to that of the bare siRNA, indicating that the presence of PMAL reduces the energy barrier and thus facilitates the transport of siRNA.

We further examined the effect of PMAL for the delivery of siRNA through the negatively charged lipid bilayer membrane, as often seen for the mammal cell membrane. As shown by Figure 3(b), the free energy barrier for pulling bare siRNA across DPPC/DPPG bilayer membrane is up to 600kJ/mol. This is attributed to the electrostatic repulsion between the siRNA and lipid bilayer membrane, both of which is negatively charged. Whereas for the complex of siRNA and PMAL, no energy barrier exists before the complex enters membrane. Instead, there is a deep energy valley of about -500kJ/mol. The substantial reduction in the energy barrier

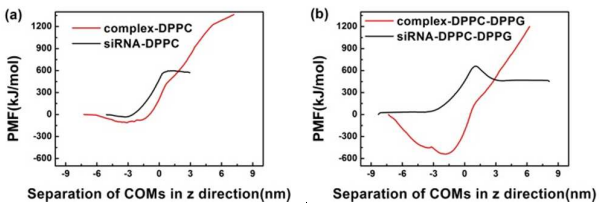

Figure 3. Free energy analysis of siRNA and siRNA-PMAL complex across cell membrane. (a) DPPC bilayer membrane; (b) DPPC-DPPG hybrid bilayer membrane, the molar ratio of DPPC and DPPG is 3 to 1, which is consistent with components of mammal cell membrane, COMs is center-of-mass.

suggests that PMAL can significantly accelerate the delivery of siRNA to the negatively charged lipid bilayer membrane.

The PMAL facilitated transport of siRNA: a process perspective

We then simulated the process of PMAL-assisted siRNA transmembrane, as shown in Figure 4.

Figure 4(a) gives the distribution of water, PMAL and lipids within 1.6nm around siRNA, as well as the distance between COMs of PMAL and of siRNA. From these time evolutions of description variables, we can divide the transmembrane process of siRNA assisted by PMAL into three stages. The first stage starts when the complex is far away from bilayer surface and ends with the complex embedded in membrane. In this stage, the proportion of PMAL around siRNA maintains constant, indicating PMAL-siRNA complex is stable during this stage. This can be further demonstrated by the distance between COMs of PMAL and siRNA, which remains constant with small fluctuation. The proportion of water around siRNA decreases while that of lipid around siRNA increases, indicating the occurrence of dehydration of the complex during embedment in lipid bilayer membrane.

The second stage starts when the complex is embedded in membrane at $t = 0.84$ μs and ends with siRNA escaping from the opposite surface of lipid bilayer membrane. In this stage, the proportion of PMAL around siRNA maintains constant, while the distance between COMs of PMAL and of siRNA increase significantly. This indicates that the structure of the PMAL-siRNA complex changes in lipid bilayer. At the same time, the proportion of water increases while that of lipid decreases. This is very interesting and is contradict to our expectations the insert of complex into lipid bilayer would be accompanied by the increase of the lipid proportion. When siRNA is moving into lipid membrane assisted by PMAL, water molecules fill the pore punched by PMAL, resulting in the increase of water around siRNA and the decrease of lipid around siRNA. This favors both the stability and delivery of siRNA.

The final stage starts with the departure of siRNA from lipid bilayer membrane and ends with separation of siRNA from lipid bilayer membrane. In this stage the portion of PMAL decreases and the distance between COMs of siRNA and of PMAL continuously increases. Meanwhile, the portion of water around siRNA increases and reaches to a plateau while the portion of lipid around siRNA decrease to zero, indicating siRNA can fully detach from lipid bilayer.

Figure 4(b) gives snapshots taken during the PMAL facilitated transport of siRNA. When $t = 0$ μs, PMAL-siRNA complex, which is above the surface of DPPC/DPPG bilayer membrane, is near-spherical with PMAL encapsulating siRNA. After 0.54 μs, the

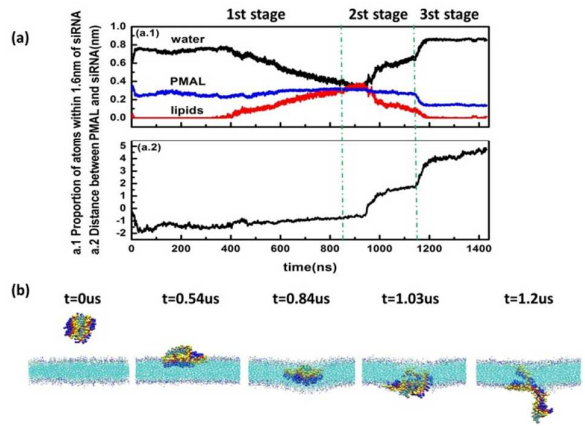

Figure 4. (a) Proportion of water , PMAL and lipids within 1.6 nm around siRNA and distance between COMs of PMAL and of siRNA; (b) Typical snapshots during PMAL-siRNA transmembrane process

complex is adsorbed on the surface of lipid bilayer and the complex deforms to exhibit ellipsoid shape. PMAL, which is amphiphilic, prefers to interact with DPPC/DPPG bilayer with both electrostatic and hydrophobic interaction. Due to the strong electrostatic interaction between siRNA and PMAL, siRNA is "forced" into lipid bilayer membrane. When $t = 0.84$ μs, siRNA totally embeds into the lipid bilayer membrane with the help of PMAL. It should be emphasized here the structure of complex embedded into lipid bilayer membrane is different from that in solution as shown in Figure 4(b) at $t = 0$ μs. The hydrophobic groups of PMAL, which are inside the complex in solution, now expose to lipid bilayer membrane due to the hydrophobic nature of lipid membrane. Once the complex moves to the opposite side of lipid bilayer membrane, i.e., $t = 1.03$ μs, siRNA leaves bilayer membrane. When the complex totally passes through bilayer membrane as shown at $t = 1.2$ μs, an elongated complex with siRNA exposed in solution

and PMAL attached on lipid membrane appears, indicating that siRNA is transported through bilayer membrane.

In order to obtain equilibrium structures of the complex at different stages of transmembrane process, molecular dynamics simulation with different initial configurations obtained from pulling simulation were performed at least for 300ns. The final structures at different stages of complex through bilayer membrane are given in Figure 5.

Figure 5(a) gives equilibrium structures of complex adsorbed on lipid bilayer surface after 300 ns traditional molecular dynamics simulations. It is shown that PMAL carries siRNA like a "boat" and the whole complex "floats" on the "lipid pool". PMAL partially adsorbs on lipid bilayer via both hydrophobic and electrostatic interaction. PMAL interacts with siRNA via electrostatic interaction. The PMAL slightly changes the density of lipid bilayer, which will be further demonstrated in Figure 6. Figure5(b) gives equilibrium structures of PMAL-siRNA complex when it totally embedded into lipid bilayer, in which PMAL tightly entangles around siRNA during extreme hydrophobic environment caused by lipid molecules. When lipid fraction around siRNA increases, PMAL fraction around siRNA also slightly increases, as shown in Figure 4(a). Figure 5(c) gives equilibrium structures of PMAL-siRNA complex when it just

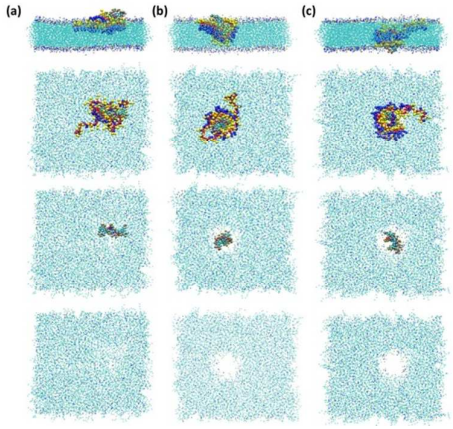

Figure 5. Typical conformations of PMAL-assisted siRNA transmembrane at different stages. (First row shows front view of siRNA-PMAL-membrane; Second row shows vertical view of siRNA-PMAL-membrane; Third row shows vertical view of siRNA-membrane; Last row shows membrane only.)

arrives at the other side of lipid bilayer membrane. The siRNA leaves the membrane while most of PMAL remains in the membrane. It is shown that "boat" totally turns over with siRNA outside lipid bilayer. The complex partially dissociates to release siRNA while PMAL is still inside lipid bilayer, which is beneficial for siRNA delivery. In conclusion, PMAL can punch on lipid bilayer and form a channel for siRNA delivery.

The PMAL facilitated transport of siRNA: a molecular structure perspective

We further studied the structural transition of siRNA, PMAL and lipids during transmembrane process, as shown in Figure 6.

Figure 6(a) gives order parameter and plane coefficient of lipid molecules of bilayer membrane during pulling simulation. It is shown that the adsorption of complex on the bilayer membrane surface doesn't cause the structural changes of lipid bilayer. Once the complex enters into membrane, the order parameter of lipid decreases while plane coefficient of lipid increases, indicating the disorder of lipid bilayer caused by the complex. Once the complex leaves bilayer membrane, order parameter of lipid recovers while plane coefficient does not. This is because PMAL still partially absorbs on the surface of lipid bilayer as shown in Figure 4(b), which affects the plane coefficient of lipid.

Figure 6(b) and (c) give radius of gyration and RMSD of siRNA, PMAL and their complex, respectively. It is shown that siRNA is very stable during transmembrane process. PMAL, however, has drastic structural changes during this process. When PMAL enters into bilayer membrane, it shrinks by reducing its gyration radius, which is caused by extrusion of lipid molecules via hydrophobic interaction. Once PMAL leaves bilayer membrane, both radius of gyration and RMSD significantly increase, indicating formation of a loose structure. The changes of complex are similar to those of PMAL, indicating the changes are mainly caused by PMAL. The major difference is that, after the complex pass through the membrane, RMSD of complex increases more than that of PMAL, indicating that siRNA escapes from complex, which is consistent with results shown in Figure 4.

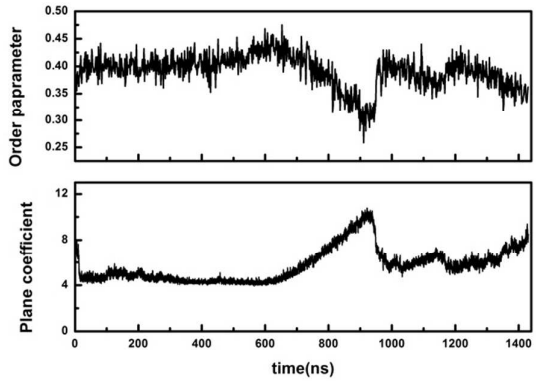

(a) Order parameter and Plane coefficient of lipid molecules change during pulling simulation

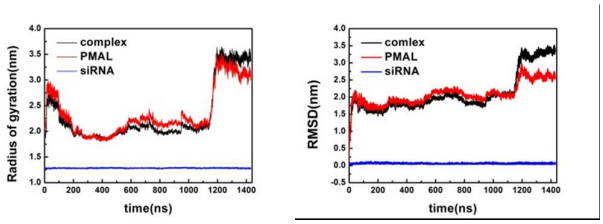

(b) Radius of gyration (c) RMSD

Figure 6. Structural transition of siRNA, PMAL and lipid bilayer during transmembrane

The PMAL facilitated transport of siRNA: experimental validation

In order to demonstrate above simulation, we fabricated liposome composed of DPPC and DPPG with the same ratio used in simulation. siRNA labelled with fluorophore and PMAL were used to detect efficiency of delivery. The molar ratio of PMAL to siRNA is 1 to 1, which is consistent with our simulation work. The results are given in Figure 7.

Figure 7(a) gives the fluorescence microscopic image in the presence of siRNA, PMAL and liposome. It is shown that although there is high fluorescence intensity in background, small dots with high green fluorescence density are visible, indicating the accumulation of siRNA in liposome. To further confirm the delivery of the complex into liposome, the sample is centrifuged to remove free siRNA, this gives an improved observation of the accumulated siRNA in liposome, i.e., the green dots, in the black background, as shown in Figure 7(b). It is thus concluded that PMAL can improve the delivery of siRNA from Figure 7.

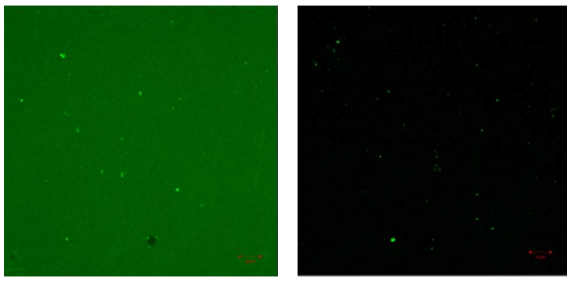

(a) Before centrifugation (b) After centrifugation

Figure 7. Detction of PMAL-assistied siRNA delivery by fluorescence microscope

Conclusions

In this work, we simulated the PMAL assisted delivery siRNA using steered molecular dynamics simulation and umbrella sampling. Potential of mean force (PMF) analyses show that energy would increase when siRNA is pulled through the membrane, indicating that delivering siRNA directly is an energy-consuming process and thus not spontaneous. In contrast, energy barrier of siRNA delivery assisted by PMAL decreases to -500kJ/mol, making the delivery process spontaneous. The simulation of the delivery process shown that that PMAL can punch on lipid bilayer and form a channel for siRNA delivery, in which the attachment of PMAL to membrane targeted siRNA towards cell membrane while the retardation of PMAL by lipid membrane facilitated the dissociation and delivery of siRNA. The experiment of PMAL-assisted siRNA through liposome further confirms the facilitated transmembrane by PMAL. The above mentioned simulation showed, at a molecular level, how PMAL displayed its function as a carrier for siRNA and thus helpful for the design and application of amphiphilic molecules for the delivery of siRNA.

Notes and references

1. L. J. Scherer and J. J. Rossi, *Nature Biotechnology*, 2003, **21**, 1457-1465.
2. G. J. Hannon, *Nature*, 2002, **418**, 244-251.
3. D. M. Dykxhoorn, C. D. Novina and P. A. Sharp, *Nature Reviews Molecular Cell Biology*, 2003, **4**, 457-467.
4. S. M. Elbashir, J. Harborth, W. Lendeckel, A. Yalcin, K. Weber and T. Tuschl, *Nature*, 2001, **411**, 494-498.
5. V. Bitko, A. Musiyenko, O. Shulyayeva and S. Barik, *Nature Medicine*, 2005, **11**, 50-55.
6. R. M. Schiffelers, A. Ansari, J. Xu, Q. Zhou, Q. Q. Tang, G. Storm, G. Molema, P. Y. Lu, P. V. Scaria and M. C. Woodle, *Nucleic Acids Research*, 2004, **32**.
7. P. L. Felgner, T. R. Gadek, M. Holm, R. Roman, H. W. Chan, M. Wenz, J. P. Northrop, G. M. Ringold and M. Danielsen, *Proceedings of the National Academy of Sciences of the United States of America*, 1987, **84**, 7413-7417.
8. D. V. Morrissey, J. A. Lockridge, L. Shaw, K. Blanchard, K. Jensen, W. Breen, K. Hartsough, L. Machemer, S. Radka, V. Jadhav, N. Vaish, S. Zinnen, C. Vargeese, K. Bowman, C. S. Shaffer, L. B. Jeffs, A. Judge, I. MacLachlan and B. Polisky, *Nature Biotechnology*, 2005, **23**, 1002-1007.
9. M. Thomas, J. J. Lu, Q. Ge, C. C. Zhang, J. Z. Chen and A. M. Klibanov, *Proceedings of the National Academy of Sciences of the United States of America*, 2005, **102**, 5679-5684.
10. O. Boussif, F. Lezoualch, M. A. Zanta, M. D. Mergny, D. Scherman, B. Demeneix and J. P. Behr, *Proceedings of the National Academy of Sciences of the United States of America*, 1995, **92**, 7297-7301.
11. J. D. Heidel, Z. P. Yu, J. Y. C. Liu, S. M. Rele, Y. C. Liang, R. K. Zeidan, D. J. Kornbrust and M. E. Davis, *Proceedings of the National Academy of Sciences of the United States of America*, 2007, **104**, 5715-5721.
12. C. X. Li, T. Y. Guo, D. Z. Zhou, Y. L. Hu, H. Zhou, S. F. Wang, J. T. Chen and Z. P. Zhang, *Journal Of Controlled Release*, 2011, **154**, 177-188.
13. J. Lisziewicz, J. Rappaport and R. Dhar, *New Biologist*, 1991, **3**, 82-89.
14. Y. Dong, K. T. Love, J. R. Dorkin, S. Sirirungruang, Y. Zhang, D. Chen, R. L. Bogorad, H. Yin, Y. Chen, A. J. Vegas, C. A. Alabi, G. Sahay, K. T. Olejnik, W. Wang, A. Schroeder, A. K. Lytton-Jean, D. J. Siegwart, A. Akinc, C. Barnes, S. A. Barros, M. Carioto, K. Fitzgerald, J. Hettinger, V. Kumar, T. I. Novobrantseva, J. Qin, W. Querbes, V. Koteliansky, R. Langer and D. G. Anderson, *Proceedings of the National Academy of Sciences of the United States of America*, 2014, **111**, 3955-3960.
15. H. Zeng, H. C. Little, T. N. Tiambeng, G. A. Williams and Z. Guan, *Journal of the American Chemical Society*, 2013, **135**, 4962-4965.
16. D. C. Forbes and N. A. Peppas, *ACS nano*, 2014, **8**, 2908-2917.
17. J. E. Dahlman, C. Barnes, O. F. Khan, A. Thiriot, S. Jhunjunwala, T. E. Shaw, Y. Xing, H. B. Sager, G. Sahay, L. Speciner, A. Bader, R. L. Bogorad, H. Yin, T. Racie, Y. Dong, S. Jiang, D. Seedorf, A. Dave, K. Singh Sandhu, M. J. Webber, T. Novobrantseva, V. M. Ruda, A. K. Lytton-Jean, C. G. Levins, B. Kalish, D. K. Mudge, M. Perez, L. Abezgauz, P. Dutta, L. Smith, K. Charisse, M. W. Kieran, K. Fitzgerald, M. Nahrendorf, D. Danino, R. M. Tuder, U. H. von Andrian, A. Akinc, D. Panigrahy, A. Schroeder, V. Koteliansky, R. Langer and D. G. Anderson, *Nature nanotechnology*, 2014, **9**, 648-655.
18. D. Meneksedag-Erol, T. Tang and H. Uludag, *Biomaterials*, 2014, **35**, 7068-7076.
19. D. Ouyang, H. Zhang, H. S. Parekh and S. C. Smith, *Biophys Chem*, 2011, **158**, 126-133.
20. K. Karatasos, P. Posocco, E. Laurini and S. Pricl, *Macromol Biosci*, 2012, **12**, 225-240.
21. L. B. Jensen, K. Mortensen, G. M. Pavan, M. R. Kasimova, D. K. Jensen, V. Gadzhyeva, H. M. Nielsen and C. Foged, *Biomacromolecules*, 2010, **11**, 3571-3577.
22. D. F. Ouyang, H. Zhang, H. S. Parekh and S. C. Smith, *J Phys Chem B*, 2010, **114**, 9231-9237.

23. C. Sun, T. Tang and H. Uludag, *Biomaterials*, 2013, **34**, 2822-2833.
24. B. M. Gorzelle, A. K. Hoffman, M. H. Keyes, D. N. Gray, D. G. Ray and C. R. Sanders, *Journal of the American Chemical Society*, 2002, **124**, 11594-11595.
25. S. J. Marrink, H. J. Risselada, S. Yefimov, D. P. Tieleman and A. H. de Vries, *J Phys Chem B*, 2007, **111**, 7812-7824.
26. J. D. Perlmutter, W. J. Drasler, W. S. Xie, J. L. Gao, J. L. Popot and J. N. Sachs, *Langmuir*, 2011, **27**, 10523-10537.
27. D. Van der Spoel, E. Lindahl, B. Hess, G. Groenhof, A. E. Mark and H. J. C. Berendsen, *Journal of Computational Chemistry*, 2005, **26**, 1701-1718.
28. W. Humphrey, A. Dalke and K. Schulten, *Journal Of Molecular Graphics & Modelling*, 1996, **14**, 33-38.
29. W. Dowhan, *Annual Review Of Biochemistry*, 1997, **66**, 199-232.
30. D. Schmidt, Q. X. Jiang and R. MacKinnon, *Nature*, 2006, **444**, 775-779.
31. S. H. Li, Y. C. Su, W. B. Luo and M. Hong, *J Phys Chem B*, 2010, **114**, 4063-4069.
32. C. Bartels, *Chemical Physics Letters*, 2000, **331**, 446-454.
33. S. Kumar, D. Bouzida, R. H. Swendsen, P. A. Kollman and J. M. Rosenberg, *Journal of Computational Chemistry*, 1992, **13**, 1011-1021.
34. H. J. C. Berendsen, J. P. M. Postma, W. F. Vangunsteren, A. Dinola and J. R. Haak, *Journal Of Chemical Physics*, 1984, **81**, 3684-3690.
35. U. Essmann, L. Perera, M. L. Berkowitz, T. Darden, H. Lee and L. G. Pedersen, *The Journal of Chemical Physics*, 1995, **103**, 8577.
36. T. Darden, D. York and L. Pedersen, *Journal Of Chemical Physics*, 1993, **98**, 10089-10092.
37. J. Q. Lin, H. W. Zhang, Z. Chen and Y. G. Zheng, *ACS nano*, 2010, **4**, 5421-5429.